Effect of Stream River and Tidal on the Suspended Sediment Concentration of Kuala Langsa Estuary, Aceh, Indonesia

Irwansyah[1]*, Faiz Isma [1], Yulina Ismida[1], Muhammad Fauzan Isma[2], Suliadi Firdaus Sufahani[3], Helmy Akbar[2,4]

[1]*Department of Civil Engineering, Faculty of Engineering, Universitas Samudra*
[2]*Department of Aquaculture, Faculty of Agriculture, Universitas Samudra*
Jl. Prof. Dr. Syarif Thayeb, Meurandeh, Langsa, Aceh, 24415 Indonesia
[3]*Statistics Programme, Faculty of Applied Sciences and Technology, Universiti Tun Hussein Onn Malaysia*
Pagoh Campus, 84600 Pagoh, Johor, Malaysia
[4]*Environmental Research Centre, IPB University*
Jl. Rasamala, Kampus IPB Darmaga Bogor 16680, West Java, Indonesia
Email: irwansyah@unsam.ac.id

Abstract

Kuala Langsa estuary is a semi-closed zone where there is an exchange of two water masses between river and tidal of the Malacca Strait. The exchange of those two water masses occurs as a physical result of fluctuating estuaries. This caused Suspended Sediment Concentration (SSC) continue to increase as the estuary is the final distribution point for sediment brought from upstream by erosion in the Langsa River. This sediment contributes to the silting of Langsa estuary. This is caused the KRI dr. Soeharso Hospital to be unable to dock at the Kuala Langsa Port during the 66th Surya Bhaskara Jaya Navy Operations 2017. It's necessary to study estuary physical conditions, which include bathymetry, currents, temperature, salinity, and concentrations of floating sediment that occur as a result of the tides and river discharges. This research used quantitative and qualitative exploratory methods, analyzed a direct correlation between the measurement results, roughness coeficient, and sediment transport rate used relevant empirical equations (Duboy's, Einstein's, Rottner, Chang, Simons, and Richardson, and Lane and Kalinske aquations). This research found that the Langsa estuary is 16 km with a semidiurnal tidal type. It was also discovered that the highest sediment rate was at the mouth of the estuary is 10.700.739,71 ton.day^{-1} and the physical model of Muara Langsa has a good correlation to the results of measurements-model indicate value of CC width = 0.959 and tide CC= 0.421, This study provides initial information for conducting hydrodynamic and morphological models at the mouth of estuary.

Keywords: *bathymetry, tidal, currents, salinity, suspended sediment concentration*

Introduction

Langsa is a part of Aceh Province and experiencing population growth and city's development. Krueng Langsa, the largest and longest river in the province, runs across in the city and end up in the port of Kuala Langsa. Following the Minister of Trade Regulation Number 24/2019, concerning the seventh amendment to Minister Regulation Number 87/M-DAG/PER/10/2015 concerning import provisions for particular products, the Kuala Langsa Port has been officially designated as an import-export port. However, the sedimentation and siltation in the port is increased from year to year. The Krueng Langsa watershed continues to experience environmental damage due to changes of land cover and land use. The port could be only become a fishing port if the sedimentation is still persisted (Fahma *et al.*, 2020). Due to shallow waters, large ships cannot dock at the port and must lean in the middle of the sea. Dredging of the estuary should be done to facilitate the entry of ships to Kuala Langsa port.

The fundamental issue of floating sediment is the dynamics of physical changes in estuaries due to tides and river discharge (Zhang *et al*., 2019; Nowacki and Grossman, 2020). Various techniques for modeling sediment transport in estuaries have been developed, especially for suspended sediments (Nerantzaki *et al.*, 2015; Higgins *et al.*, 2016; Zettam *et al.*, 2017; Gan *et al.*, 2018; Li *et al.*, 2018; Liu *et al.*, 2019; Moreira and Simionato, 2019; Basri *et al.*, 2020; Nowacki and Grossman, 2020). Those studies have successfully modeled the physical system in the long stretch of the estuary, including changes in water depth, tides, currents, temperature, salinity, and sediment concentration. When the basic

*) Corresponding author

https://ejournal.undip.ac.id/index.php/ijms
DOI: 10.14710/ik.ijms.28.1.27-36
Received : 20-01-2022
Accepted : 08-09-2022

understanding of the estuary characteristics has been obtained and validated against field data from the physical estuary, the robustness of the model could be confirmed. This study determines the effect of water level fluctuations on the physical system of Kuala Langsa estuary. Validations were done to confirm the robustness of the model. The model were then compared with the measurement data based on the validation of numerical models that have been carried out by Temmerman *et al.* (2004) and Nurzahziani and Surussavadee (2018).

Material and Methods

The research site was the Kuala Langsa estuary, and it has been observed that salinity reached approximatelly 1 mg.l^{-1} from the mouth of Muara Langsa to the upstream. There are 17 stations (Station A-Q) along the river with 1 km apart between station (Figure 1.). This research used quantitative and qualitative exploratory methods. Tidal was measured every 15 days in Station A (Pusong Island). Water samples were taken at a depth of 0.2, 0.6 and 0.8 d using a Van Dorn horizontal water sampler and analyzed for suspended sediment content. The bottom sediment was collected using a Grab Sampler subjected to laboratory testing to obtain the grain size of the sediment.

Currents were measured using a current meter was divided by five segments based on the cross-sectional width of the estuary for each station using the one-point method for shallow waters with depth (d) less than 2 m (0.6 d) and the two-point method for deep waters (0.2 d and 0, 8 d) and depth measurement using Garmin 585 GPS linked with coordinates and depth sensor.

The total discharge is determined by equation (1) with the average flow velocity carried out by direct measurement.

$$Q = \bar{V} x\, A \qquad (1)$$

Note: Q is discharge (m^{3}s^{-1}); V is velocity (ms^{-1}); A is area (m^2). Average flow velocity was calculated with the following equation (SNI, 2015).

One point method:

$$\bar{V} = V_{0.6} \qquad (2)$$

Two point method:

$$\bar{V} = \frac{V_{0.2}+V_{0.6}}{2} \qquad (3)$$

Note: $V_{0,2}$ is flow rate at depth 0.2 h and $V_{0,6}$ is flow rate at depth 0.6 h

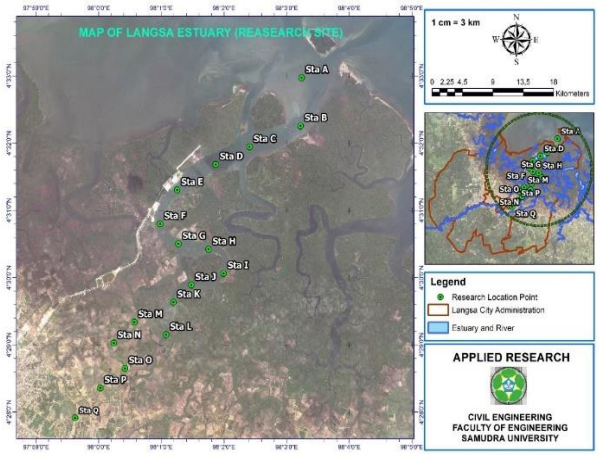

Figure 1. The location of data collection in the Langsa estuary

The process of sediment transportation was distinguished based on the movement of the sediment grain. Sediment rate can be determined from the sediment grains movement due to flow velocity, which consists of base sediment rate, suspended sediment, and total sediment. The base sediment rate was predicted using Duboy's (1979) equation, Van Rijn, and Rottner's equation (1959).

Duboy's equation (1979) assumes that sediment particles move in layers along the bottom of the flow. This layer moves because of the traction force works. The thickness of each layer (τ) in stable conditions and the tractive force must be balanced by the total resistivity force between layers. Determination of critical traction force at the base (τ_c) was performed using the Shield diagram. The following is the sediment parameters and critical traction force for the Duboy's bedload equation (Metric unit).

$$q_b = \frac{0{,}173}{d^{0{,}75}}\, \tau\, (\tau - \tau_c) \qquad (4)$$

Note: d is the diameter of the sediment particles that 50% pass the sieve.

The rate of base sediment load (Bed Load) was predicted using Van Rijn equation as follows.

$$q_b = \frac{0{,}173}{d^{0{,}75}}\, \tau\, (\tau - \tau_c) \qquad (5)$$

Rottner (1959) states the basic sediment rate of inflow parameter term is based on dimensional considerations and regression analysis to produce the effect of the relative roughness parameter d50/D as follows.

$$qb = \rho s\, [(\zeta s - 1) g\, D^3]^{1/2}\, X \left\{ \frac{V}{[(\zeta s-1) gD]^{1/2}} \left[0.667 \left(\frac{d_{50}}{D} \right)^{2/3} + 0.14 \right] - 0.778 \left(\frac{d_{50}}{D} \right)^{2/3} \right\}^3 \qquad (6)$$

Note: qb is bed load discharge (m^3/s), s is sediment mass density ($kg.m^{-3}$), ζ_s is sediment specific gravity ($kg.m^{-3}$), g= gravity ($m.s^{-2}$), V= average velocity mean ($m.s^{-1}$) and d_{50} = diameter of sediment particles that pass 50% of the sieve (m).

The suspended sediment rate was predicted by the equation of Lane and Kalinske, Einstein's equation, and Chang, Simons, and Richardson expressed in Yang (1996). The suspended sediment concentration was measured using Standard Test Method D 3977-97 (ASTM) according to Guy (1969). Then the suspended sediment rate was determined using the Lane and Kalinske equation as follows.

$$q_{sw} = q\ Ca\ P_L\ exp\ (\frac{15\omega a}{U*D}) \qquad (7)$$

Note: qsw is the weight of the sediment per unit time and width; q is the flow rate per unit width ($m^3.s^{-1}$); PL is a function of $\bar{C}/C_a$ stated C is the integrated average sediment concentration and ω = Falling speed according to D_{50} as follows.

$$\omega = \left[\frac{g.d^2}{18\ v}\right]\left(\frac{\gamma_s}{\gamma}\right) \qquad (8)$$

Note: ω is sediment fall velocity ($m.s^{-1}$); *v* is the coefficient of kinematic viscosity with a value of 1.10-6 (Stoke's Law); g is Earth's gravity (9.81 $m.s^{-1}$); d is Diameter of sediment passing sieve 50%; γ_s is the density of sediment is the density of water (62.4 $lb.ft^{-3}$ or 1000 $kg.m^{-3}$) (U.S. Bureau of Reclamation, 1987)

Einstein's equation assumes that the charge is floating. Chang Simons and Richardson Equation are estimated by corresponding to the average of dry drifting sediment in estuary water bodies. Formzahl numbers is determinants of tidal types in estuaries (Work *et al.*, 2013). Einstein's equation is as follows:

$$q_{sw} = 11{,}6\ U'_*\ C_a\ a\left[\left(2{,}303\ log\ \frac{30{,}2\ D}{\Delta}\right) I_1 + I_2\right] \quad (9)$$

Note: Δ is d_{65} / *x* and X is obtained from the comparison graph $\frac{k_s}{\delta'}$ in (Yang, 1996).

Tidal classification states: if F ≤ 0.25 (double daily/semidiurnal types), if 0.25< F ≤ 1.5 (semidiurnal skewed mix), 1.5<F≤3.0 (diurnal skewed mixed type), F> 3.0 (diurnal daily type).

The formation of a numerical model of the physical estuary with a computational program was done through equations given by Hardisty (2007), *i.e*. (a) Bathymetry, numerical model obtained by determining the depth of flow (d) and the width of estuary by exponential difference of the starting point of observation from the (river) mouth to the upstream divided every 1 km distance in the measurement to produce a geometric shape. (b) High and low tides. The amplitude components of the tidal measurement data every 15 days were used to determine the type of tide using formzal numbers. The tidal harmonic function causes changes in the depth of the estuary with time, h(t) of the estuary. (c) Temperature and salinity. The condition of temperature and salinity was varied in each measuring point (TX). The salinity of each measuring point (SX) can be calculated using the Gauss distribution equation (Isma *et al.*, 2020) . (d) Suspended sediment concentration (SSC). Because of reciprocate of tide and river flows in estuaries, the floating of sediment will change according to the time (hour). Channel roughness factor affects the flow. The effect of flow velocity and depth on channel roughness is determined by observation of bottom sediment grain diameter and field flow velocity in each point using the following equation. Manning's roughness coefficient (1889):

V = 1 / nx R2 / 3 S1 / 2 (Metric) or
$V = 1,49 / n\ x\ R^{2/3}\ x\ S^{1/2}$ (10)

Raudkivi roughness coefficient (1971):

$n = 0.42\ h1 / 6$ or $n = 0.013 D_{65}^{1/6}$ (11)

Muller's roughness coefficient: $n = \frac{D_{90}^{1/6}}{26}$

Note: n is the value of the roughness of the manning coefficient (dimensionless); R is the open channel hydraulic radius (m); S is the slope of the longitudinal channel (%), and V is the velocity ($m.s^{-1}$); D65 is a grain diameter of which 65% of the grain fraction passes through the filter; D90 is a grain diameter of which 90% of the grain fraction passes through the filter.

The result of the roughness coefficient from the 3 equations above then were analyzed by performing a simple linear regression model, Y=a+bX to predict the roughness coefficient equation (n). This equation is used in the estuary conditions of the Langsa estuary by examining the correlation (r) between the results of the roughness coefficient and the depth (d) so regression model is n= a + bd and velocity (v) so regression model is n= a + bv in the estuary. The correlation equation is used to check the suitability of the roughness coefficient formula approach used for the cross-section of the estuary (Fasdarsyah, 2017).

Results and Discussion

The characteristics of the sediment at the mouth of the estuary varied, i.e. fine sand to silt with an average grain diameter of 0.7786 mm. The

sediment transport rate at the mouth of the estuary is the highest in table 1 indicating that the upstream estuary is unstable. The value of sediment sorting distributed in the middle platform was <0.25 with a very well sorted level. Right and left sorting ranges from 0.5 to 1.0 with uniformity of medium disaggregated sediments (Figure 3.). The sediment transport rate at Sta Q (upstream) was 0.073 $kg.s^{-1}.m^{-1}$ or 167.68 $tons.day^{-1}$ spread over a width of 25 m and a depth of 1.84 m. The condition of sediment rate at this station is low in residential areas. On the other hand, the highest sediment rate occurred in the downstream of the estuary, i.e. in Station A at 1.07 x 107 $tons.day^{-1}$ spread over a width of 1,809 m and a depth of 8.26 m as shown in Table 1.

The tidal data drawn using the admiralty method obtained K_1 component of 3.45 cm, O_1 of 2.05 cm, S_2 of 14.25 cm, and M_2 of 32.63 cm, resulting in formzahl number (F) value of 0.12<0,25 (Figure 2.). Thus, the Langsa estuary has a semidiurnal tidal type (Figure 2.). Based on the Numerical modeling of tides, the correlation between measurements model has a CC value of 0.830. These results show that there is a correlation between the measurement for estuarine tidal events with ME -6.06 and RMSE of 25.12 as shown in Table 2.

Table 3 explains the magnitude of the roughness coefficient that occurred at the bottom of the Langsa river estuary where the minimum value produced was 0.003274 in the Raudkivi equation and the maximum value was 0.9759 based on the Manning equation. Meanwhile, the minimum value obtained from the Manning equation was 0.06942. This result is similar with research of Zevri (2021) in the Meulaboh estuary and produced the Formzahl number 0.19 that is associated to the semidiurnal tidal type. According to Tarigan *et al.* (2017), the physical model of the Belawan estuary also demonstrated a semidiurnal tidal type. The physical model exponentially produced a good relationship between the depth and width of the Belawan estuary and the maximum and minimum currents near the mid-tide and low tide obtained regression equation between roughness and depth coefficients is n= 0,004 + 1,0 x 10^{-5} d (middle channel) and Regression equation The roughness coefficient of tidal currents is n = 0,004 + 1,0 x 10^{-5} v (middle channel).

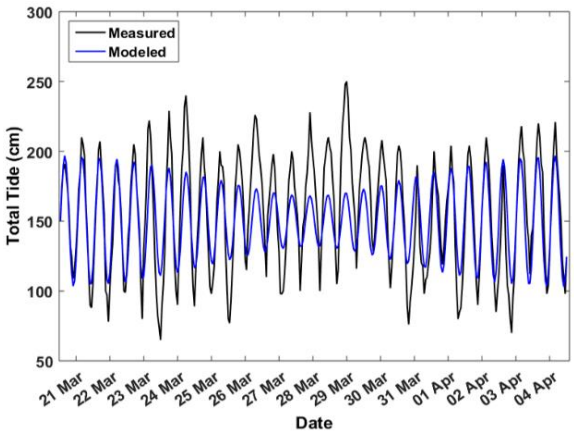

Figure 2. The Correlation of tidal measurements and models

Table 1. Overpass and basic sediment transport rate in Langsa Estuary

Location	Q ($m^3.s^{-1}$)	Suspended Load Rate			Bed Load Rate			Total rate ($ton.day^{-1}$)
		Lane and Kalinske $kg.s^{-1}.m^{-1}$	*Einstein* $kg.s^{-1}.m^{-1}$	*Chang, Simons and Richardson* $kg.s^{-1}.m^{-1}$	*DuBoy'* $kg.s^{-1}.m^{-1}$	*Van Rijn* $kg.s^{-1}.m^{-1}$	*Rottner* ($kg.s^{-1}.m^{-1}$)	
STA A	3,563.29	1.2499	0.0112	0,0008	0.0000	65.016	-0.00098	10.700.739,71
STA C	1,208.57	0.9378	0.0000	0.0000	0.0000	0.718	-	81.983,92
STA E	1,944.98	0.0030	0.0000	0.0001	0.0000	0.742	-	20.432,04
STA G	1,900.60	0.0208	0.0000	0.0001	0.0001	13.843	-	458.776,40
STA I	1,208.53	0.2343	0.0001	−0.0004	0.0000	134.186	-0.01549	3.774.513,60
STA K	78.76	0.0138	0,0002	−0.0001	0.0000	0.963	-	19.499,36
STA M	34.89	0,0003	0,0005	−0.0001	0.0000	0.156	-	1.266,97
STA O	10.36	0,0001	0.0000	−0.0001	0.0000	0.0081	-	39,40
STA Q	12.36	0,0002	0.0000	−0.0001	0.0000	0.073	-0.01530	157,68

However, based on the provisions given by Manning, it was found that the channel conditions were winding, clean, curved, and cliffs with a minimum value of 0.0333 and a maximum value of 0.045 (Fasdarsyah, 2017). it varies with conditions of the Kuala Langsa estuary has a tremendous depth and width that affects the hydraulic radius. The value of the roughness coefficient was then correlated with the conditions of the estuary depth and tide currents. The maximum current velocity at ebb was 0.06075 $m.s^{-1}$ 0.06075 $m.s^{-1}$ located at Sta G with a depth of 9.44878. The maximum current velocity at tide was 0.04225 $m.s^{-1}$, which is also at Sta G and coincides with the mangrove area. This location is used for measuring the tides of the Krueng Langsa estuary, where it leads to the bend of the estuary. This is in accordance to the river legislation, which states that erosion often occurs in the outside turn area, while the turn in area is prone to deposition/sedimentation (Christine, 2009).

The correlation coefficient of roughness to the depth and tidal currents of Krueng Langsa estuary is described in Table 3. The results explain that the correlation between the coefficient of roughness and the depth of the estuary obtained based on the Manning equation is most suitable to be applied with the value of CC 0.655 with the highest correlation (r) of 0.809, which produced a regression model of n= 0.394 + 0.076 d. When viewed from the current correlation condition from tide to ebb, the most suitable based on the Muler equation is CC= 0.598, where the correlation (r) value was 0.7733 and the regression model was n= 0.011 + 0.009 h. Meanwhile, the flow from the ebb to tide correlation was found to be insignificant with the largest CC value of 0.309 with a correlation (r) of 0.560 in the Jarrett equation, which had a regression model of n= 0.021 - 0.061 h. In the Muler equation, CC for tidal flow was 0.214 with a correlation (r) of 0.463. Based on these results, the depth correlation according to the Manning equation for estuary waters matches with research by Farsdarsyah (2017) in the Lhoksukon River. In those research, the correlation between the roughness coefficient and the depth of the Lhoksukon River had R of 0.66 with a regression model of n= 0.0137 d - 0.0016, indicating that manning is suitable to use in open channels with deep waters such as estuaries and rivers.

The physical parameters, the depth and width of the Langsa estuary were modeled. This model was then compared with the measurement data in Table 2. Based on Table 2, it is known that the measurement of the estuary with a width (W0) of 1,860 m and a depth (D0) of 8,264 m obtained a width coefficient of (a) 6, 03 and depth (b) of 1.48, which was obtained from the physical numerical model of the estuary referring to (Isma *et al.*, 2020). These results indicate that there is a good relationship between measurements-model indicated by the value of CC width = 0.959 and depth CC= 0.421 as shown in Table 2.

Based on the findings of this research, the Langsa estuary has the highest depth variation at Sta J, which is located 9 km from the estuary (mouth) of 23.38 m and the pier area at Sta E has a depth of 21.03 m, which is higher than the depth at the estuary mouth (Table 4.). Hence, it was demonstrated that the silting Langsa estuary has a sediment transport rate of 66,65,016 $kg.s^{-1}.m^{-1}$, with the Engelund and Hansen equations having the the highest sediment rate of the 3 equations and Lines and Kalinske having the highest elevation sediment rate of 1,250 $kg.m^{-1}.s^{-1}$ (Table 1.).

In this case, the rate of sediment transport becomes polemic in the estuary because this location is the confluence of tidal currents and river discharge. The highest sediment transport rate found was 134,420 $kg.s^{-1}.m^{-1}$ at Sta I or 8 km from the mouth of the estuary with a width of 325 m and obtained a sediment transport of 43,686.50 $kg.s^{-1}$, while a sediment rate of 0.073 $kg.s^{-1}.m^{-1}$ with a width of 25 m was found in the upstream part of Sta Q (16 km from the estuary of the estuary). The sediment rate upstream of the estuary was 157.68 $tons.day^{-1}$. This is due to the small grains of sediment that can move in that location, indicating that sediment has been transported to the mouth of the estuary because the sediment rate at the mouth of the estuary was high at 10,700,739.71 $tons.day^{-1}$. In the end, it was stated that estuary Langsa estuary had the most extensive sediment transport rate at each observed station.

Table 2. The Correlation between models - measurements of the physical parameters of estuarine estates

Parameter	Koef.	ME	RMSE	CC
Width	6.030	-29.790	159.340	0.958
Depth	1.480	-5.110	8.020	0.420
Temperature	10.620	0.090	0.270	0.963
Salinity	11.190	-2.070	3.980	0.942
Tide	-	-6.060	25.120	0.830

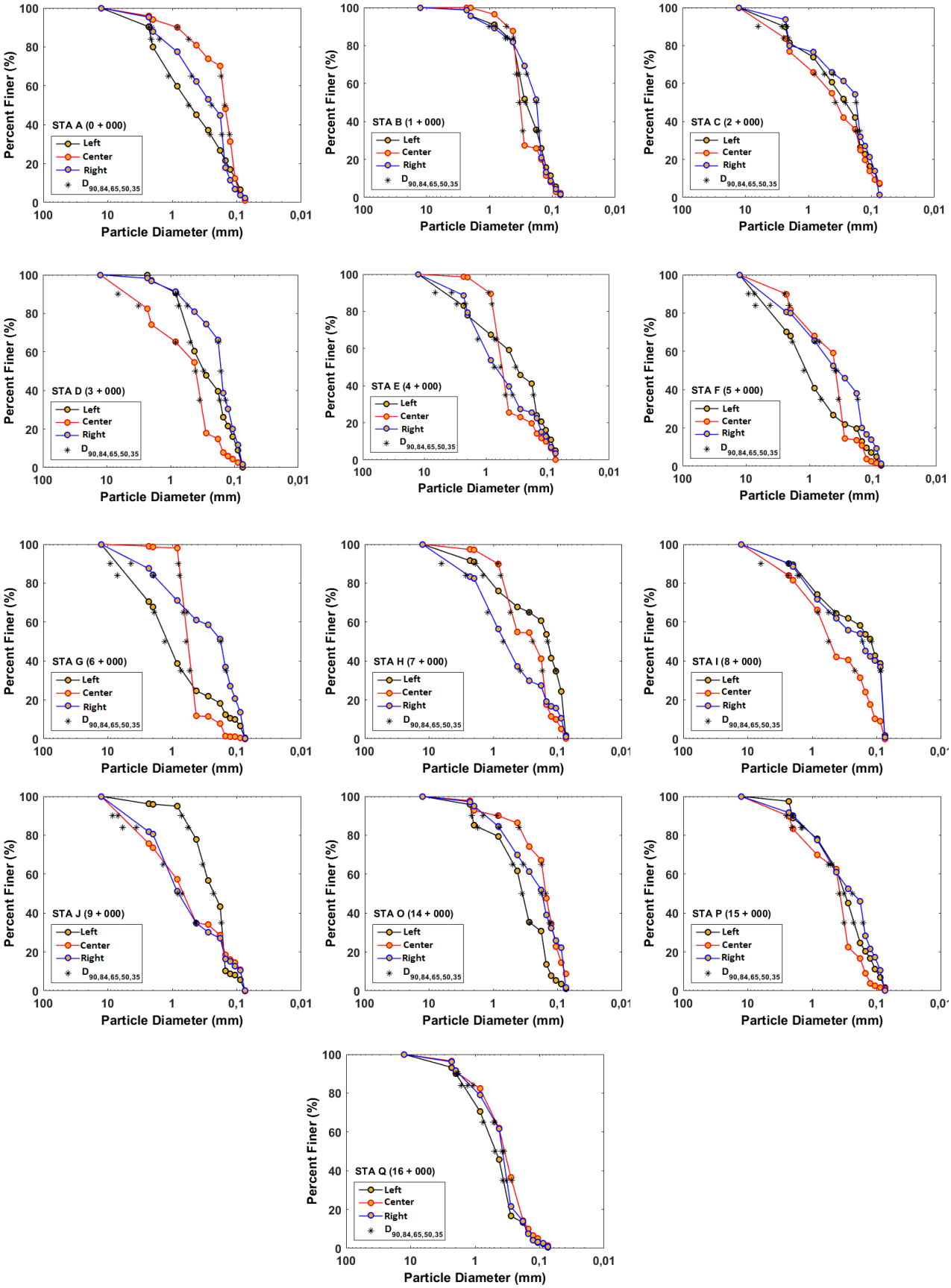

Figure 3. Grain size Curve

Table 3. The Correlation of Roughness and Depth and Estuary Flow.

No.	Formulation	Part	Regression equation between roughness and depth coefficients	r
1	MULER	Left	$n = 0{,}013 + 9 \times 10^{-5} d$	0,076
		Middle	$n = 0{,}014 + 3{,}3 \times 10^{-7} d$	0,00000242
		Right	$n = 0{,}013 + 1{,}9 \times 10^{-4} d$	0,257
2	MANNING	Left	$n = - 0{,}108 + 0{,}167 d$	0,390
		Middle	$n = 0{,}004 + 1{,}0 \times 10^{-5} d$	0,655
		Right	$n = 0{,}137 + 0{,}123 d$	0,409
3	RAUDKIVI	Left	$n = 0{,}004 + 1{,}1 \times 10^{-4} d$	0,099
		Middle	$n = 0{,}004 + 1{,}0 \times 10^{-5} d$	0,068
		Right	$n = 0{,}003 + 5{,}0 \times 10^{-5} d$	0,269
No	Formulation	Part	Regression equation The roughness coefficient of tidal currents	r
1	MANNING	Left	$n = 0{,}534 + 2{,}096 v$	0.037
		Middle	$n = 0{,}004 + 1{,}0 \times 10^{-5} v$	0,655
		Right	$n = 0{,}804 + 1{,}616 v$	0.063
2	RAUDKIVI	Left	$n = 0{,}003 + 0{,}001 v$	0.216
		Middle	$n = 0{,}003 + 0{,}001 v$	0.155
		Right	$n = 0{,}003 + 0{,}002 v$	0.501
3	MULER	Left	$n = 0{,}012 + 0{,}007 v$	0.261
		Middle	$n = 0{,}013 + 0{,}0004 v$	0.001
		Right	$n = 0{,}011 + 0{,}009 v$	0.598

Table 4. Measurement of physical parameters of the estuary in the field

Measurement Station	Width (m)	Depth (m)	Temperature (°C)	Salinity (‰)	SSC (kg.m^{-3})
A (0 + 000)	1869	8.26	29.95	38.00	0.379
B (1 + 000)	1002	2.09	30.18	37.90	0.421
C (2 + 000)	573	7.91	30.40	37.35	0.436
D (3 + 000)	456	13.29	30.75	37.95	0.434
E (4 + 000)	317	21.03	31.10	37.25	0.439
F (5 + 000)	284	17.76	31.40	37.35	0.336
G (6 + 000)	383	9,70	31.45	37.00	0.358
H (7 + 000)	220	17.58	31.41	36.45	0.408
I (8 + 000)	325	9.30	31.55	35.40	0.428
J (9 + 000)	295	23.38	31.58	34.95	0.420
K (10 + 000)	231	8.36	31.85	31.80	0.416
L (11 + 000)	197	3.68	31.98	27.95	0.384
M (12 + 000)	94	3.29	31.95	25.10	0.337
N (13 + 000)	76	2.32	31.95	19.35	0.304
O (14 + 000)	57	2.26	32.08	16.85	0.302
P (15 + 000)	45	1.95	31.96	14.95	0.307
Q (16 + 000)	25	1.84	32.08	7.85	0.298

The measurement results presented in Table 4 show that the range of tides in the Langsa estuary was 16 km from the mouth of the estuary. Sea temperature is cooler than river temperature, which is in line with the statement (Hardisty, 2007) and the concentration of suspended solids towards the mouth of the estuary tends to be higher than towards the river. This indicates a high sediment movement downstream of the Langsa estuary. The correlation of the movement of depth, temperature, and salinity with time due to tidal and tidal fluctuations is shown in Figure 4.

However, the occurrence of suspended sediment continues to change caused by the current and tidal factors and river discharges along the estuary. Figure 3 describes the changes in suspended solids every hour along with fluctuations of current at high tide and low tide. This shows that at low tide the suspended solid concentration in the estuary upstream water body has increased. Due to river discharge in the estuary's upstream part, tidal currents from the estuary cross-section will produce changes in the SSC content. Figure 3, in this case, states that at the lowest tide, the SSC content will increase.

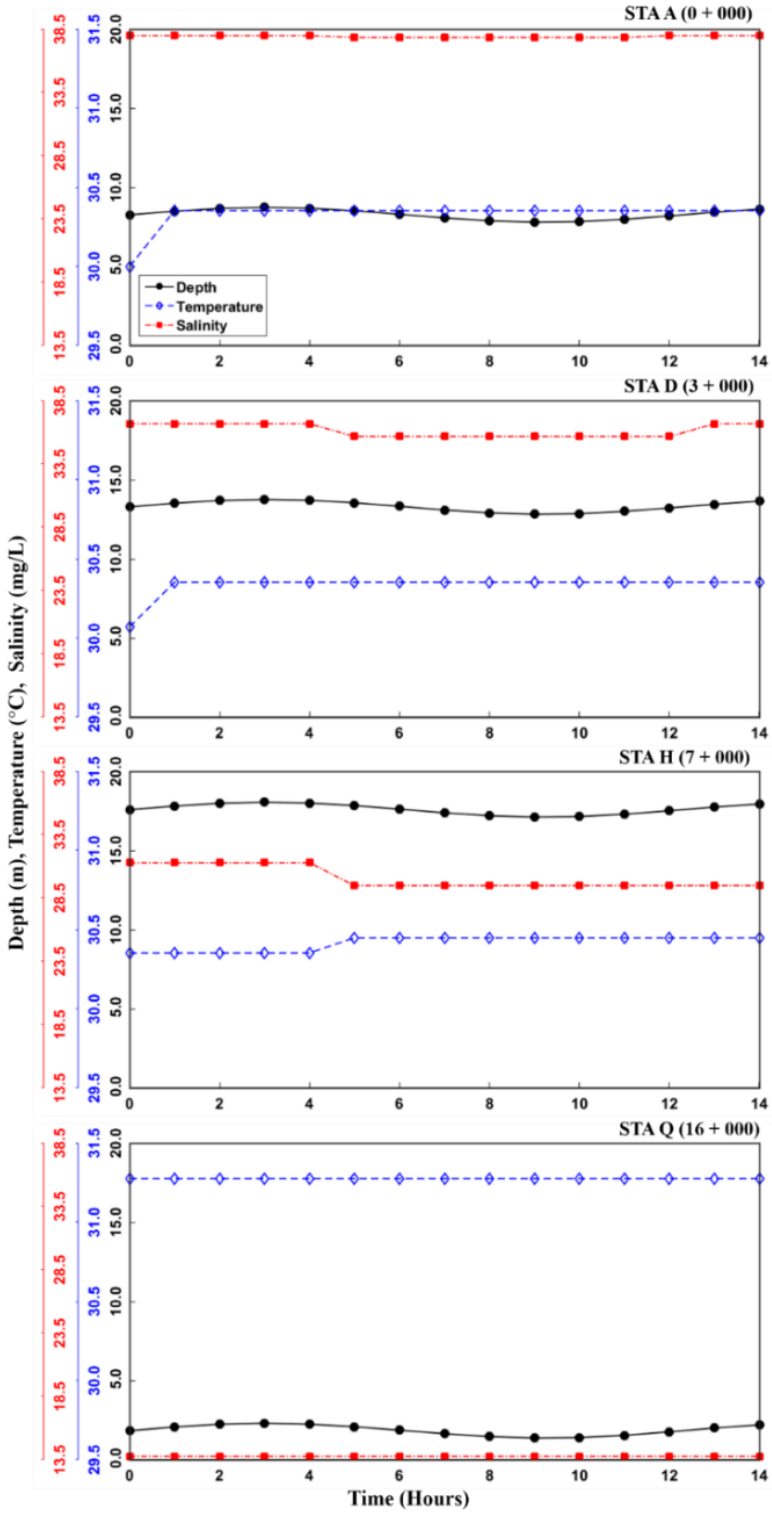

Figure 4. The Correlation of Depth (m), Temperature (°C), and Salinity (mg.l^{-1}) with time (h).

As a basis for the next study, further research is needed on the hydrodynamic model of sediment transport to see the sedimentation pattern that occurs at the mouth of the Langsa estuary and its effect on the occurrence of degradation in the Langsa watershed.

Conclusion

The tidal range extends upstream 6 km from the mouth of the estuary. Sediment characteristics towards the mouth of the estuary tend to be higher than the direction of the river. It can be seen that the dynamics of sediment transport occurs at the mouth of the estuary, which has the potential to cause silting at the mouth of the estuary. The average distribution of sediment grains in the middle pyramid is 0.2613 and is included in the sand category. Meanwhile, the value of the sorting of sediments scattered in the middle pyramid has a value of about <0.25 with a very good level of uniformity of sorting. The highest sedimentation rate based on the results of this study is 1.07 x 107 tons.day^{-1} at the mouth of the estuary, which is estimated to be the cause of silting at the mouth of the estuary at this time.

Acknowledgements

This research was financed by Community Service and Research Center (LPPM) in cooperation with Applied Research Program through DIPA Samudra University Academic Year 2019 in Contract Agreement Number 313/UN54.6/LT/201.

References

[ASTM] American Society for Testing and Materials. 2000. Standard test methods for determining sediment concentration in water samples: D3977-97, 11 (2), Water (II): 395-400.

Basri, H., Azmeri, A., Wesli, W. & Jemi, F.Z. 2020. Simulation of Sediment Transport in Krueng Baro River, Indonesia, *Jamba: J. Disaster Risk Studies*, 12(1): 1–9. https://doi.org/10.4102/JAMBA.V12I1.934

Christine, M. 2009. Pembentukan kelokan sungai. *Majalah Ilmiah Maranatha*, 16(2): 34-46

Fahma, B., Siregar, N., Isma, F. & Lydia, N. 2020. Study of Basic Sediment Transport in the Kuala Langsa Estuary, *Media Tek. Sipil Samudra*, 1(1): 1–6

Fasdarsyah, F. 2017. Analisis Karakteristik Sedimen Dasar Sungai Terhadap Parameter Kedalaman, *Teras J.*, 6(2): 91-100. https://doi.org/10.29103/tj.v6i2.108

Gan, B.R., Liu, X.N., Yang, X.G., Wang, X.K. & Zhou, J.W. 2018. The Impact of Human Activities on the Occurrence of Mountain Flood Hazards: Lessons from the 17 August 2015 Flash Flood/Debris Flow Event in Xuyong County, South-Western China. *Geomat. Nat. Hazards Risk.,* 9(1): 816–40 https://doi.org/10.1080/19475705.2018.1480539

Hardisty, J. 2007. Estuaries: Monitoring and Modeling the Physical System, Blackwell Publishing. https://doi.org/10.1002/9780470 750889

Higgins, A., Restrepo, J.C., Ortiz, J.C., Pierini, J. & Otero, L., 2016. Suspended sediment transport in the Magdalena River (Colombia, South America): Hydrologic regime, rating parameters and effective discharge variability. *Int. J. Sediment Res.*, 31(1): 25-35. https://doi.org/10.1016/j.ijsrc.2015.04.003

Isma, F., Ismida, Y., Purwandito, M. & Fajri, H., 2020, Numerical modeling of suspended sediment concentration (SSC) due to water surface fluctuations of the Krueng Langsa estuary, Aceh Province, *IOP Conf. Ser. Materials Sci. Eng.*, 933(1): p. 012022. https://doi.org/10.1088/1757-899X/933/1/012022.

Li, L., He, Z., Xia, Y. & Dou, X., 2018. Dynamics of sediment transport and stratification in Changjiang River Estuary, China. *Estuar., Coast. Shelf Sci.*, 213: 1-17. https://doi.org/10.1016/j.ecss.2018.08.002

Liu, J., Xu, Z., Chen, F., Chen, F. & Zhang, L., 2019. Flood hazard mapping and assessment on the Angkor world heritage site, Cambodia. *Remote Sensing*, 11(1): p.98. https://doi.org/10.3390/rs1 1010098

Moreira, D. & Simionato, C.G., 2019. Modeling the suspended sediment transport in a very wide, shallow, and microtidal estuary, the Río de la Plata, Argentina. *J. Adv. Model. Earth Syst.*, 11(10): 3284-3304. https://doi.org/10.1029/2018MS001605

Nerantzaki, S.D., Giannakis, G.V., Efstathiou, D., Nikolaidis, N.P., Sibetheros, I.A., Karatzas, G.P. & Zacharias, I., 2015. Modeling suspended sediment transport and assessing the impacts of climate change in a karstic Mediterranean watershed. *Sci. Total Environ.*, *538*: 288-297.https://doi.org/10.1016/j.scitotenv.2015.07.092

Nowacki, D.J. & Grossman, E.E., 2020. Sediment transport in a restored, river-influenced Pacific Northwest estuary. *Estuar. Coast. Shelf Sci.,*

242: p.106869. https://doi.org/10.1016/j.ecss.2020.106869

Nurzahziani & Surussavadee, C. 2018. Numerical Simulations for Biomass Burning Aerosol Transport in Northern Thailand, *IOP Conf. Ser.: Earth Environ. Sci.*, 164(1): p.012008. https://doi.org/10.1088/1755-1315/164/1/012008

Tarigan, A.P.M., Swandana, D. & Isma, F. 2017. Modelling the Physical System of Belawan Estuary, *IOP Conf. Ser.: Materials Sci. Eng.*, 180(1): p.012124. https://doi.org/10.1088/1757-899X/180/1/012124

SNI, 2015. Tata cara pengukuran debit aliran sungai dan saluran terbuka menggunakan alat ukur arus dan pelampung, Badan Standarisasi Nasional. Republik Indonesia.

Tarigan, A.P.M., Swandana, D. & Isma, F. 2017. Modelling the Physical System of Belawan Estuary, *IOP Conf. Ser.: Materials Sci. Eng.*, 180(1): p.012124. https://doi.org/10.1088/1757-899X/180/1/012124

Temmerman, S., Govers, G., Wartel, S. & Meire, P., 2004. Modelling estuarine variations in tidal marsh sedimentation: response to changing sea level and suspended sediment concentrations. *Mar. Geolog.*, 212(1-4): 1-19. https://doi.org/10.1016/j.margeo.2004.10.021

Work, P.A., Haas, K.A., Defne, Z. & Gay, T. 2013. Tidal stream energy site assessment via three-dimensional model and measurements. *Applied energy*, 102: 510-519. https://doi.org/10.1016/j.apenergy.2012.08.040

Yang, C.T. 1996. Sediment Transport Theory and Practice (McGraw – Hill, Singapore.

Zettam, A., Taleb, A., Sauvage, S., Boithias, L., Belaidi, N. & Sánchez-Pérez, J.M. 2017. Modelling hydrology and sediment transport in a semi-arid and anthropized catchment using the SWAT model: The case of the Tafna river (northwest Algeria). *Water*, 9(3): p.216. https://doi.org/10.3390/w9030216

Zevri, A. 2021. Studi Potensi Daerah Genangan Banjir Pasang (Rob) Perairan Meilaboh Dengan Sistem Informasi Geografis (Kajian Teknis), *J. Teoritis Terapan Bidang Rekayasa Sipil*, 28(3): 371–80. https://doi.org/10.5614/ jts.2021.28.3.14